# High Rate, Selective, and Stable Electroreduction of CO$_2$ to CO in Basic and Neutral Media

Cao-Thang Dinh,[†,§] F. Pelayo García de Arquer,[†,§] David Sinton,[‡] and Edward H. Sargent*[,†]

[†]Department of Electrical and Computer Engineering, University of Toronto, 10 King's College Road, Toronto, ON, Canada, M5S 3G4

[‡]Department of Mechanical and Industrial Engineering, University of Toronto, 5 King's College Road, Toronto, ON, Canada, M5S 3G8

S Supporting Information

ABSTRACT: The electroreduction of carbon dioxide (CO$_2$) to chemicals such as carbon monoxide (CO) shows great potential for renewable fuel and chemical production. Significant progress in individual performance metrics such as reaction rate, selectivity, and stability has been achieved, yet the simultaneous achievement of each of these key metrics within a single system, and in a wide range of operating conditions, has yet to be demonstrated. Here we report a composite multilayered porous electrode consisting of a polytetrafluoroethylene gas distribution layer, a conformal Ag catalyst, and a carbon current distributor. Separating the gas and current distribution functions provides endurance, and further reconstructing the catalyst to carbonate-derived Ag provides flexibility in terms of electrolyte. The resulting electrodes reduce CO$_2$ to CO with a Faradaic efficiency over 90% at current densities above 150 mA/cm^2, in both neutral and alkaline media for over 100 h of operation. This represents an important step toward the deployment of CO$_2$ electroduction systems using electrolyzer technologies.
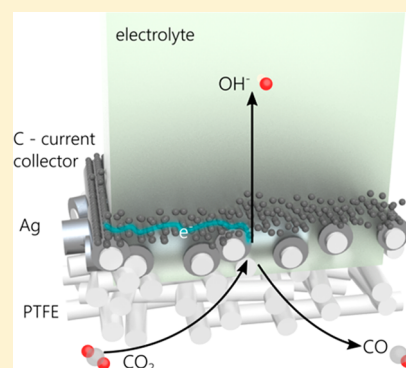
The electroreduction of carbon dioxide (CO$_2$) to chemicals represents a promising pathway for the storage of renewable electricity and toward low-carbon-footprint chemicals production.[1,2] Out of the various products that can be produced from CO$_2$ electrochemical reduction reaction (CO$_2$RR), carbon monoxide (CO) is a particularly versatile precursor, extensively used for the production of several chemicals such as methanol and synthetic fuels.[3,4] In addition, the two-electron transfer required to reduce CO$_2$ into CO provides a large profit margin compared to other multiple-electron transfer products, which require larger electricity energy inputs.[4,5] With these advantages, carbon monoxide is uniquely well-positioned as a commercial CO$_2$RR product, provided the conversion performance metrics can be met.

High selective (Faradaic efficiency up to 90%) CO$_2$RR to CO has been demonstrated on various catalysts, such as Ag,[6] Au,[7] Cu,[2] Pd,[8] MoS$_2$,[9] and WSe$_2$,[10] using an aqueous electrolyzer (H-cell) system. The stability of some of these catalysts has been demonstrated for testing times longer than 10 h[3] but generally with current densities below 10 mA/cm^2 for CO$_2$RR to CO. Higher current densities have been achieved through electrode nanostructuring.[6,11] However, due to the low solubility of CO$_2$ in aqueous electrolyte and long

diffusion distance, the current densities remained below 30 mA/cm^2—far from the >100 mA/cm^2 regime needed to make CO$_2$RR electroreduction to CO economically viable.[12,13]

Gas-phase CO$_2$RR offers a path to overcome the diffusion limitation of aqueous CO$_2$RR, thereby enabling higher current density.[13] In a gas-phase CO$_2$RR system, the catalyst is deposited onto a porous hydrophobic substrate (gas diffusion layer), greatly reducing the required CO$_2$ diffusion length and accelerating mass transport. Using a gas diffusion layer, current densities up to a few hundreds of mA/cm^2 have been achieved with alkaline electrolyzer and bipolar membrane electrolyzer configurations. However, the simultaneous fulfillment of high CO selectivity and long stability at high current densities has yet to be demonstrated.

In the alkaline electrolyzer configuration, the catholyte can be either basic or neutral. When a basic electrolyte such as KOH is used, CO selectivity above 90% can be obtained.[14−16] In addition, the alkaline media reduces the CO$_2$RR over-potential, resulting in a higher energy efficiency.[17] However,
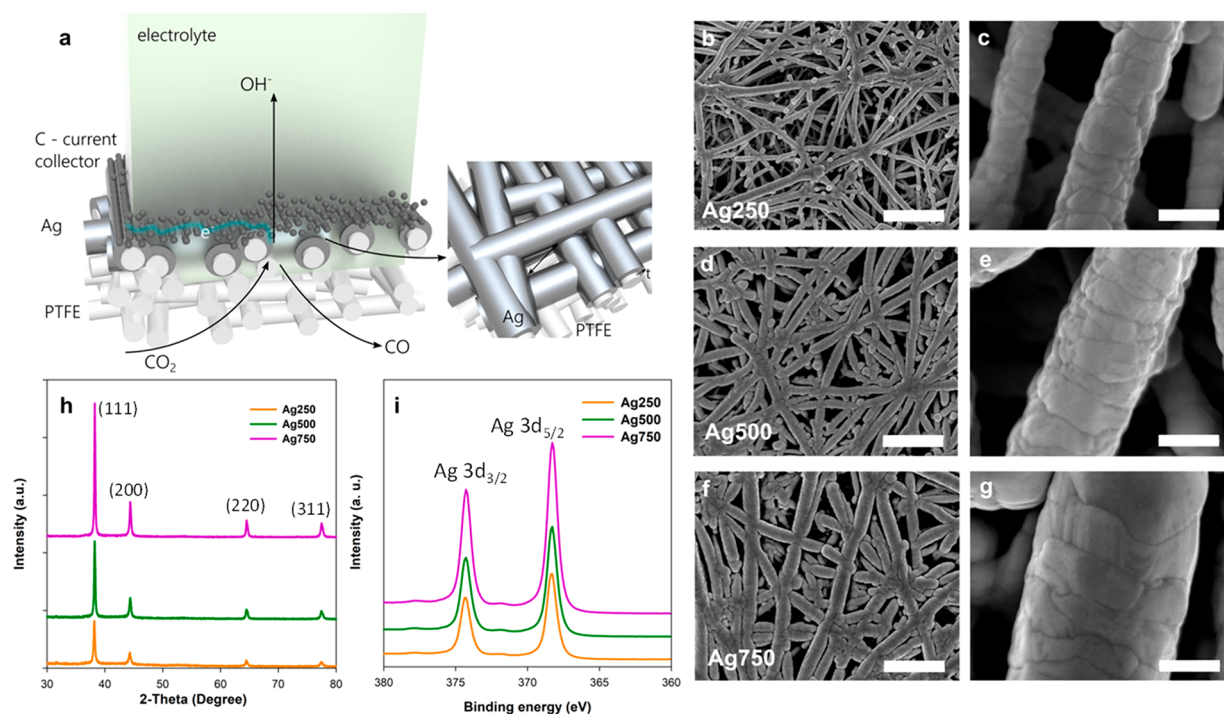
Figure 1. Electrode design and characterization. (a) Illustration of the designed electrode composed of PTFE membrane, conformal Ag catalyst, and carbon nanoparticle current distributor. (b−g) SEM characterization of Ag/PTFE membrane with a nominal thickness of 250 nm (Ag250, b and c); 500 nm (Ag500, d and e); and 750 nm (Ag750, f and g). (h) XRD and (i) XPS characteriztions of Ag/PTFE catalyst with varying thickness. The scale bars in parts b, d, and f are 2500 nm, and those in parts c, e, and g are 250 nm.

the use of basic media poses significant stability challenges for the catalyst and the gas diffusion electrode. For example, the carbon-based gas diffusion electrode was found to degrade over 2 h in basic electrolyte during both CO_2 and CO reduction reactions.[18,19] Thus, long-term CO_2RR to CO in alkaline media has not been demonstrated to date.

To overcome the limited stability in alkaline media, a neutral electrolyte combined with a flow-through electrode configuration has been demonstrated.[20] This flow-through structure overcame electrode flooding arising from the deactivated hydrophobicity of the substrate but at the expense of decreased CO selectivity at high current density.[20] A modified proton-exchange-membrane configuration[21] and bipolar membrane electrolyzers operating under neutral conditions have also been explored to overcome the limited stability for CO_2RR, leading to a stability of more than 24 h at a current density of 100 mA/cm^2, albeit with a CO selectivity of ∼70%.[13,22−24]

In summary, present-day CO_2RR electrolyzers that can operate at high current density have been reported in either neutral or basic media. However, achieving high current density, high selectivity, and high stability under these two conditions remains an unresolved challenge.

Here we report the design and demonstration of a C/Ag/PTFE composite electrode consisting of (i) a porous PTFE membrane that stabilizes the gas diffusion electrode in basic media; (ii) an active Ag catalyst that selectively reduces CO_2 to CO in both neutral and basic electrolyte; and (iii) a carbon nanoparticle layer that distributes current on the surface of Ag catalyst. We engineer this system to achieve high CO Faradaic efficiency (>90%), achieve high current density (>150 mA/cm^2), and retain this performance for an extended testing period (>100 h) in both neutral and basic media.

The composite CO_2RR cathode electrode consists of three layers: a porous PTFE membrane; the Ag catalyst coated on the surface of PTFE; and black carbon nanoparticles coated on the surface of Ag catalysts (Figure 1a). Here, the non-conductive PTFE membrane serves as the gas diffusion layer as opposed to a porous and conductive carbon-based gas diffusion layer traditionally employed for CO_2RR. A conformal, continuous Ag layer combined with the porous carbon layer provides a uniform current distribution for CO_2RR. Thus, the roles of the gas diffusion layer and current distributor are decoupled in our electrode design, with the aim to eliminate the issue of flooding in carbon-based gas diffusion layers.

To fabricate the electrode, we first sputtered the Ag catalyst on a PTFE membrane (450 nm pore size) with a tunable thickness. The nominal thickness of Ag was varied between 250, 500, and 750 nm. A carbon nanoparticle solution was then sprayed to establish the current collector.

We first characterized the composite electrodes using scanning electron microscopy (SEM) before carbon deposition. The Ag/PTFE exhibits a wire structure where Ag is continuously and conformally grown on PTFE wires and throughout the PTFE membrane (Figure 1b−g). Higher Ag loading increases the diameter of the wires and reduces the pore size of the electrode. The Ag grain size slightly increased with increasing deposition thickness (Figure 1d, e, and g). After carbon coating, the electrode surface is porous, covering the entire Ag/PTFE surface (Figure S1).

We characterized the oxidation state of the Ag catalysts using X-ray photoelectron spectroscopy (XPS). The oxidation state of Ag in all samples was zero, indicating a pure metallic character that does not depend on deposition thickness (Figure 1i). We further characterized the crystallinity of the samples using X-ray diffraction (XRD), which confirmed the
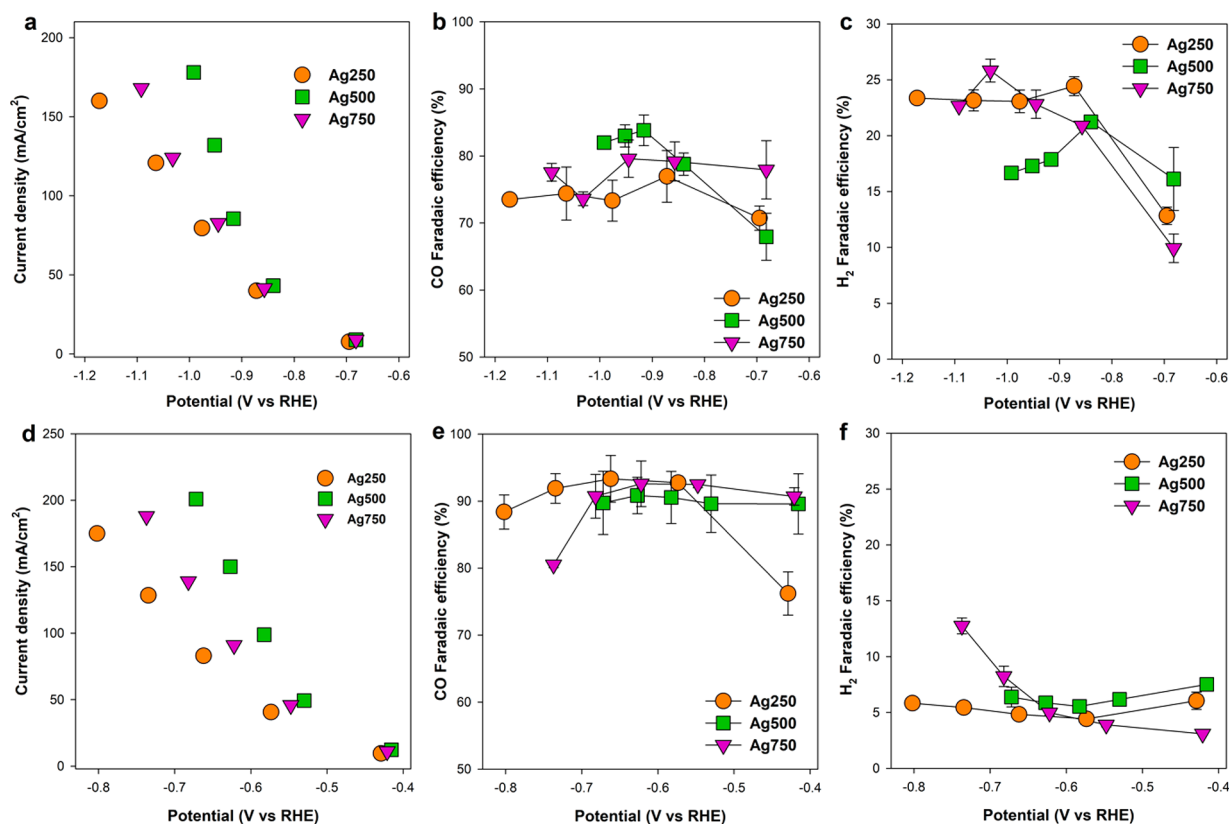
Figure 2. CO_2RR performance of Ag/PTFE catalysts in neutral and basic electrolyte. (a−c) Neutral electrolyte performance vs applied potential in terms of current density (a), CO Faradaic efficiency (b), and H_2 Faradaic efficiency (c) in 1 M $KHCO_3$ electrolyte, with catalyst thicknesses indicated. (d−f) Basic electrolyte performance vs applied potential, similarly, in terms of current density (d), CO Faradaic efficiency (e), and H_2 Faradaic efficiency (f). All samples were coated with carbon nanoparticles for CO_2RR measurements.

metallic phase of Ag in all samples (Figure 1h). The width of the XRD peaks decreased with increasing deposition thickness, indicating a larger grain size for thicker samples which is in a good agreement with SEM observation.

We first monitored the dependence of current density on applied potential in neutral electrolyte (1 M $KHCO_3$) using three different Ag catalysts (Figure 2a). CO_2-RR performance was evaluated in a flow cell configuration using the same electrolyte for both the cathode and anode chambers, which were separated by an anion exchange membrane.[19] The Ag catalyst with a thickness of 500 nm (Ag500) exhibited the highest current density, highlighting the importance of the balance between Ag loading and electrode pore size to achieve high current density. At an applied potential of −1 V vs RHE, Ag500 shows a current density up to 175 mA/cm^2. All three catalysts exhibited an average CO Faradaic efficiency of 70−80% in the potential range from −0.7 to −1.2 V vs RHE, indicating that sputtered Ag/PTFE does not selectively reduce CO_2 to CO in neutral media. The H_2 Faradaic efficiency was in the range 15−25% for all samples, leading to a total CO and H_2 Faradaic efficiency close to 100%. Liquid product analysis using the NMR method on a representative sample confirmed formate as the only liquid product with a Faradaic efficiency below 2% (Figure S2).

We then sought to test the performance of the Ag composite catalyst in alkaline media (1 M KOH). Similar current densities were observed for all samples but at lower applied potentials owing to the higher CO_2RR activity in the alkaline media (Figure 2d). A similar trend was observed in alkaline electrolyte with Ag500 exhibiting the highest current density,

with 200 mA/cm^2 at −0.7 V vs RHE. In contrast to neutral electrolyte, all Ag/PTFE catalysts exhibited a high CO Faradaic efficiency of 90% at most of the applied potentials (Figure 2e). H_2 formation was suppressed to the range 5−7% for both Ag250 and Ag500 (Figure 2f). Ag750 showed a high H_2 Faradaic efficiency at high current density, which could be attributed to the small pore size limiting the diffusion of CO_2 to the catalyst surface in alkaline media. Liquid product analyses of Ag500 at the applied potentials of −0.5 to −0.7 V vs RHE confirmed formic acid as the remaining product, with a Faradaic efficiency of 3−5% (Figure S3).

Although the Ag/PTFE catalysts exhibit high CO selectivity in alkaline media, their CO selectivity in neutral electrolyte remains around 80% in most of the applied potentials. To further improve CO selectivity in neutral media, we sought to reconstruct the surface of Ag catalyst using an electrochemical oxidation−reduction process to form oxide/carbonate-derived catalysts.[25,26] Oxide/carbonate-derived Ag catalysts have been found to be selective catalysts for CO_2 reduction to CO at low current density (<10 mA/cm^2).[25,26] However, the performance of oxide/carbonate-derived Ag catalyst at high current density has not been demonstrated.

To form carbonate-derived Ag/PTFE catalyst (CD-Ag/PTFE), we performed repeated CV cycles (three cycles) on Ag/PTFE (Ag500) in the potential range from −0.8 to +1.3 V vs Ag/AgCl in 1 M $KHCO_3$ electrolyte (Figure 3a). The surface of the catalyst changed from dense Ag/PTFE to nanoporous Ag/PTFE with a smooth surface and a particle size range of 30−100 nm (Figure 3b and Figure S4). The Ag 3d XP spectrum of CD-Ag/PTFE did not show any shift
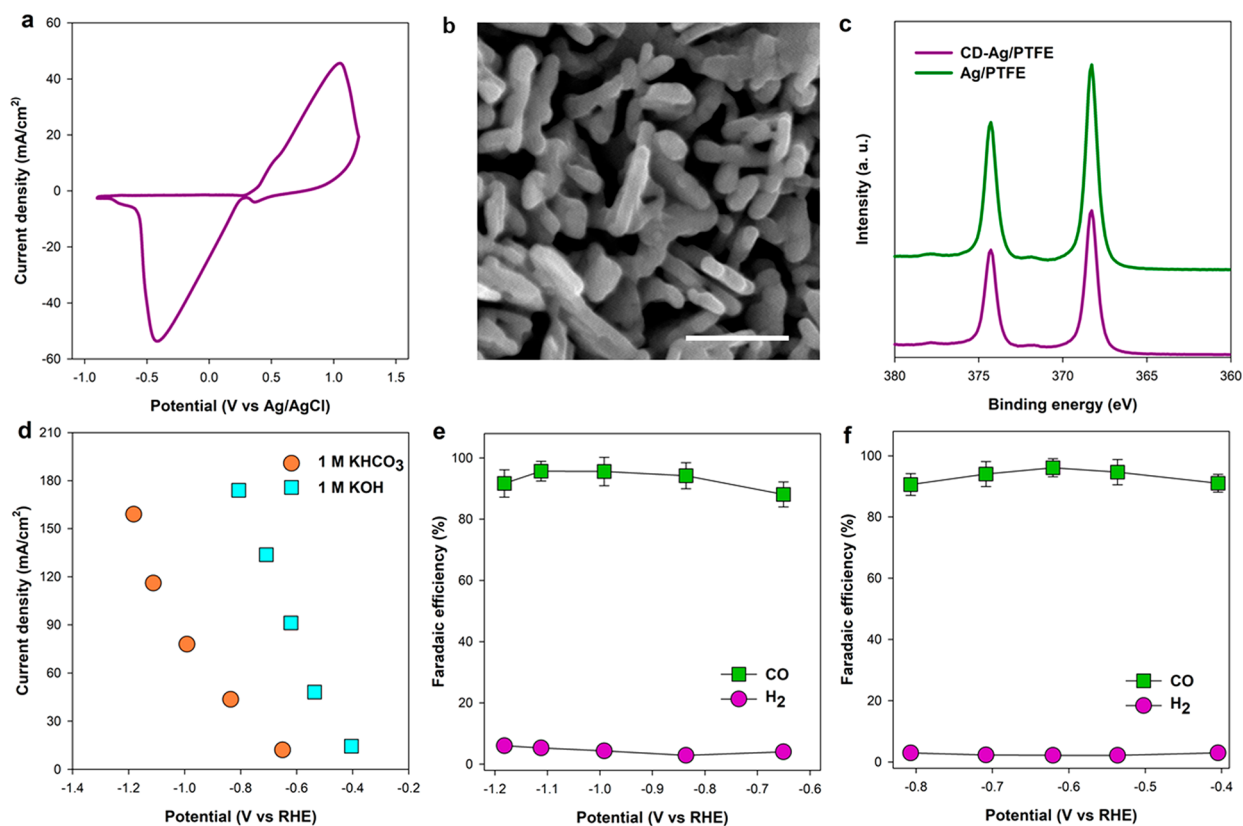
Figure 3. Characterization and CO_2RR performance of carbonate-derived, CD-Ag/PTFE, catalyst. (a) A representative CV curve for the oxidation−reduction of Ag/PTFE catalyst to form CD-Ag/PTFE catalyst. (b) SEM and (c) XPS characterization of CD-Ag/PTFE catalyst (shown here without the carbon nanoparticles used during CO_2RR measurements). (d) Total current density vs applied potential over CD-Ag/PTFE catalyst in 1 M $KHCO_3$ and 1 M KOH electrolytes. CO and H_2 Faradaic efficiency at different applied potentials in 1 M $KHCO_3$ electrolyte (e) and 1 M KOH electrolyte (f). The scale bar in part b is 200 nm.

compared to that of metallic Ag/PTFE, confirming the formation of a pure metallic Ag phase after three repeated CV cycles (Figure 3c). The XRD results of CD-Ag/PTFE (Figure S5) further confirm the metallic crystalline structure of Ag in this sample. However, compared to pristine Ag/PTFE, the CD-Ag/PTFE exhibited wider XRD peaks, indicating a smaller grain size.

The CO_2RR performance of CD-Ag/PTFE catalyst was tested in both neutral (1 M $KHCO_3$) and basic (1 M KOH) electrolytes. Compared to Ag/PTFE catalyst, CD-Ag/PTFE exhibited similar current densities in the potential range of −0.6 to −1.1 V vs RHE with both neutral and basic electrolytes (Figure 3e). In contrast to current density, the CO Faradaic efficiency on CD-Ag/PTFE was much higher (>90%) compared to that on Ag/PTFE in neutral electrolyte across the whole potential range studied. In basic electrolyte, CD-Ag/PTFE also showed a high CO selectivity of >92% for all current densities between 10 and 170 mA/cm² (Figure 3f).

Previous studies have shown two different effects that could lead to enhanced CO_2RR performance of oxide/carbonate-derived Ag catalysts at a low current density (<10 mA/cm²): (i) a local change in the pH induced by the higher surface area and porous structure; (ii) an electronic reconfiguration induced by a surface morphology change.[25−27] The increase in the local pH induced by the high current density suppresses H_2 evolution favoring the reduction of CO_2, thereby leading to an increase in CO selectivity.[28] The electronic reconfiguration resulting from the surface morphology reconstruction would lead to a change in the binding energy of CO_2RR

intermediates, lowering the activation energy barrier for CO_2RR to CO.

In this study, we investigated CO_2RR over a wide current density range from 10 to 200 mA/cm² where the local pH varies significantly. However, we did not observe a significant improvement in CO selectivity for all Ag/PTFE catalysts in this current density range (Figures 2b and 3e). In addition, both Ag/PTFE and CD-Ag/PTFE exhibited similar current densities at the same applied potentials, indicating a similar local pH for both Ag/PTFE and CD-Ag/PTFE. These results suggest that the local pH may not play a significant role in enhancing the CO selectivity for CD-Ag/PTFE catalysts at this high current density range. Instead, we found a significant change in the morphology of Ag/PTFE catalyst after the oxidation−reduction process, which may lead to different crystal facets being exposed, and enhanced CO selectivity akin to that observed in nanoporous Ag.[6,26]

To study the stability of CD-Ag/PTFE catalyst in both neutral and basic media at high current density (>150 mA/cm²), we performed long-term CO_2RR at a fixed potential of −1 V vs RHE in 1 M $KHCO_3$ electrolyte (Figure 4a) and of −0.7 V vs RHE in 1 M KOH electrolyte (Figure 4b). The CD-Ag/PTFE catalyst exhibited stable current densities in the range 150−170 mA/cm² in neutral electrolyte for an extended testing time over 100 h. In basic electrolyte, a slight decrease in current density from 180 to 150 mA/cm² was observed after 24 h of continuous runtime. This current density decrease is attributed to the reduction of electrolyte conductivity caused by the transformation of KOH to carbonate salt in the
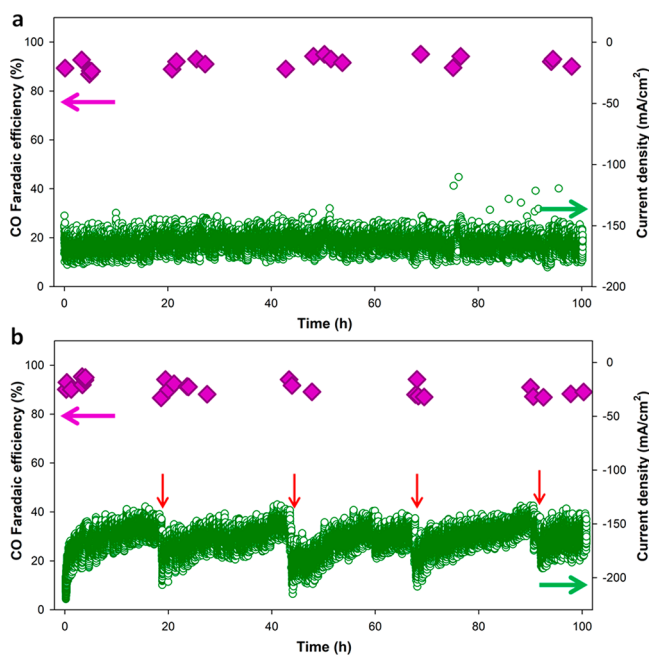
Figure 4. Long-term stability test of CD-Ag/PTFE catalyst in neutral and basic media. The stability of CO Faradaic efficiency and current density versus time on CD-Ag/PTFE catalysts in 1 M $KHCO_3$ electrolyte (a) and 1 M KOH electrolyte (b). The red arrows in part b indicate the times at which the electrolyte in the cathode was refreshed.

electrolyte. The current density was restored when the electrolyte was refreshed (Figure 4b). More importantly, CO selectivities were maintained at >90% throughout the run in both neutral and basic media, demonstrating the high stability of the CD-Ag/PTFE catalyst. These performance metrics surpass those of previously reported catalysts at a similar high current density range (Table S1) and represent an essential advance in the maturity of electrocatalytic CO_2 to CO conversion technology.

In summary, we demonstrated an Ag composite catalyst electrode strategy for selective and stable electroreduction of CO_2 to CO at high current density in both basic and neutral media. We combine a PTFE gas diffusion electrode with selective carbonate-derived Ag catalyst to achieve a CO selectivity of >90% at a current density of >150 mA/cm^2 for a long-term testing time of 100 h. These high performance metrics were achieved in both $KHCO_3$ and KOH electrolytes, opening the door for the implementation of these catalysts in various electrolyzer configurations including bipolar membrane and alkaline-based electrolyzers for viable CO_2RR.

ASSOCIATED CONTENT

Ⓢ Supporting Information

The Supporting Information is available free of charge on the ACS Publications website at DOI: 10.1021/acsenergy-lett.8b01734.

Experimental details and additional data (PDF)

AUTHOR INFORMATION

Corresponding Author

*E-mail: ted.sargent@utoronto.ca.

ORCID Ⓞ

Cao-Thang Dinh: 0000-0001-9641-9815

David Sinton: 0000-0003-2714-6408

Edward H. Sargent: 0000-0003-0396-6495

Author Contributions

§C.-T.D., F.P.G.d.A.: These authors contributed equally to this work.

Notes

The authors declare no competing financial interest.

ACKNOWLEDGMENTS

REFERENCES

(1) Lin, S.; Diercks, C. S.; Zhang, Y.-B.; Kornienko, N.; Nichols, E. M.; Zhao, Y.; Paris, A. R.; Kim, D.; Yang, P.; Yaghi, O. M.; et al. Covalent Organic Frameworks Comprising Cobalt Porphyrins For Catalytic CO_2 Reduction in Water. *Science* **2015**, *349*, 1208−1213.

(2) Schreier, M.; Héroguel, F.; Steier, L.; Ahmad, S.; Luterbacher, J. S.; Mayer, M. T.; Luo, J.; Grätzel, M. Solar Conversion of CO_2 to CO using Earth-Abundant Electrocatalysts Prepared by Atomic Layer Modification Of CuO. *Nat. Energy* **2017**, *2*, 17087.

(3) Hernández, S.; Amin Farkhondehfal, M.; Sastre, F.; Makkee, M.; Saracco, G.; Russo, N. Syngas Production from Electrochemical Reduction Of CO_2: Current Status and Prospective Implementation. *Green Chem.* **2017**, *19*, 2326−2346.

(4) Verma, S.; Kim, B.; Jhong, H.-R. M.; Ma, S.; Kenis, P. J. A. A Gross-Margin Model for Defining Technoeconomic Benchmarks in the Electroreduction of CO_2. *ChemSusChem* **2016**, *9*, 1972−1979.

(5) Bushuyev, O. S.; De Luna, P.; Dinh, C. T.; Tao, L.; Saur, G.; van de Lagemaat, J.; Kelley, S. O.; Sargent, E. H. What Should We Make with CO_2 and How Can We Make It? *Joule* **2018**, *2*, 825−832.

(6) Lu, Q.; Rosen, J.; Zhou, Y.; Hutchings, G. S.; Kimmel, Y. C.; Chen, J. G.; Jiao, F. A Selective and Efficient Electrocatalyst for Carbon Dioxide Reduction. *Nat. Commun.* **2014**, *5*, 3242.

(7) Chen, Y.; Li, C. W.; Kanan, M. W. Aqueous CO_2 Reduction at Very Low Overpotential on Oxide-Derived Au Nanoparticles. *J. Am. Chem. Soc.* **2012**, *134*, 19969−19972.

(8) Gao, D.; Zhou, H.; Wang, J.; Miao, S.; Yang, F.; Wang, G.; Wang, J.; Bao, X. Size-Dependent Electrocatalytic Reduction of CO_2 over Pd Nanoparticles. *J. Am. Chem. Soc.* **2015**, *137*, 4288−4291.

(9) Asadi, M.; Kumar, B.; Behranginia, A.; Rosen, B. A.; Baskin, A.; Repnin, N.; Pisasale, D.; Phillips, P.; Zhu, W.; Haasch, R.; et al. Robust Carbon Dioxide Reduction on Molybdenum Disulphide Edges. *Nat. Commun.* **2014**, *5*, 4470.

(10) Asadi, M.; Kim, K.; Liu, C.; Addepalli, A. V.; Abbasi, P.; Yasaei, P.; Phillips, P.; Behranginia, A.; Cerrato, J. M.; Haasch, R.; et al. Nanostructured Transition Metal Dichalcogenide Electrocatalysts for CO_2 Reduction in Ionic Liquid. *Science* **2016**, *353*, 467−470.

(11) Liu, M.; Pang, Y.; Zhang, B.; De Luna, P.; Voznyy, O.; Xu, J.; Zheng, X.; Dinh, C. T.; Fan, F.; Cao, C.; et al. Enhanced Electrocatalytic CO_2 Reduction via Field-Induced Reagent Concentration. *Nature* **2016**, *537*, 382.

(12) Singh, M. R.; Goodpaster, J. D.; Weber, A. Z.; Head-Gordon, M.; Bell, A. T. Mechanistic Insights into Electrochemical Reduction Of CO_2 over Ag using Density Functional Theory and Transport Models. *Proc. Natl. Acad. Sci. U. S. A.* **2017**, *114*, E8812−E8821.

(13) Weekes, D. M.; Salvatore, D. A.; Reyes, A.; Huang, A.; Berlinguette, C. P. Electrolytic CO_2 Reduction in a Flow Cell. *Acc. Chem. Res.* **2018**, *51*, 910−918.

(14) Verma, S.; Lu, X.; Ma, S.; Masel, R. I.; Kenis, P. J. A. The Effect of Electrolyte Composition on the Electroreduction of CO_2 to CO on

Ag based Gas Diffusion Electrodes. *Phys. Chem. Chem. Phys.* **2016**, *18*, 7075−7084.

(15) Ma, S.; Luo, R.; Gold, J. I.; Yu, A. Z.; Kim, B.; Kenis, P. J. A. Carbon Nanotube Containing Ag Catalyst Layers for Efficient and Selective Reduction of Carbon Dioxide. *J. Mater. Chem. A* **2016**, *4*, 8573−8578.

(16) Verma, S.; Hamasaki, Y.; Kim, C.; Huang, W.; Lu, S.; Jhong, H.-R. M.; Gewirth, A. A.; Fujigaya, T.; Nakashima, N.; Kenis, P. J. A. Insights into the Low Overpotential Electroreduction of CO_2 to CO on a Supported Gold Catalyst in an Alkaline Flow Electrolyzer. *ACS Energy Lett.* **2018**, *3*, 193−198.

(17) Gabardo, C. M.; Seifitokaldani, A.; Edwards, J. P.; Dinh, C.-T.; Burdyny, T.; Kibria, M. G.; O'Brien, C. P.; Sargent, E. H.; Sinton, D. Combined High Alkalinity and Pressurization Enable Efficient CO_2 Electroreduction to CO. *Energy Environ. Sci.* **2018**, *11*, 2531−2539.

(18) Jouny, M.; Luc, W.; Jiao, F. High-Rate Electroreduction of Carbon Monoxide to Multi-Carbon Products. *Nat. Catal.* **2018**, *1*, 748−755.

(19) Dinh, C.-T.; Burdyny, T.; Kibria, M. G.; Seifitokaldani, A.; Gabardo, C. M.; García de Arquer, F. P.; Kiani, A.; Edwards, J. P.; De Luna, P.; Bushuyev, O. S.; et al. CO_2 Electroreduction To Ethylene via Hydroxide-Mediated Copper Catalysis at an Abrupt Interface. *Science* **2018**, *360*, 783−787.

(20) Haas, T.; Krause, R.; Weber, R.; Demler, M.; Schmid, G. Technical Photosynthesis Involving CO_2 Electrolysis and Fermentation. *Nat. Catal.* **2018**, *1*, 32−39.

(21) Delacourt, C.; Ridgway, P. L.; Kerr, J. B.; Newman, J. Design of an Electrochemical Cell Making Syngas $(CO + H_2)$ from CO_2 and H_2O Reduction at Room Temperature. *J. Electrochem. Soc.* **2008**, *155*, B42−B49.

(22) Salvatore, D. A.; Weekes, D. M.; He, J.; Dettelbach, K. E.; Li, Y. C.; Mallouk, T. E.; Berlinguette, C. P. Electrolysis of Gaseous CO_2 to CO in a Flow Cell with a Bipolar Membrane. *ACS Energy Lett.* **2018**, *3*, 149−154.

(23) Li, Y. C.; Zhou, D.; Yan, Z.; Gonçalves, R. H.; Salvatore, D. A.; Berlinguette, C. P.; Mallouk, T. E. Electrolysis of CO_2 to Syngas in Bipolar Membrane-Based Electrochemical Cells. *ACS Energy Lett.* **2016**, *1*, 1149−1153.

(24) Vermaas, D. A.; Smith, W. A. Synergistic Electrochemical CO_2 Reduction and Water Oxidation with a Bipolar Membrane. *ACS Energy Lett.* **2016**, *1*, 1143−1148.

(25) Ma, M.; Trześniewski, B. J.; Xie, J.; Smith, W. A. Selective and Efficient Reduction of Carbon Dioxide to Carbon Monoxide on Oxide-Derived Nanostructured Silver Electrocatalysts. *Angew. Chem., Int. Ed.* **2016**, *55*, 9748−9752.

(26) Ma, M.; Liu, K.; Shen, J.; Kas, R.; Smith, W. A. In Situ Fabrication and Reactivation of Highly Selective and Stable Ag Catalysts for Electrochemical CO_2 Conversion. *ACS Energy Lett.* **2018**, *3*, 1301−1306.

(27) Rosen, J.; Hutchings, G. S.; Lu, Q.; Rivera, S.; Zhou, Y.; Vlachos, D. G.; Jiao, F. Mechanistic Insights into the Electrochemical Reduction of CO_2 to CO on Nanostructured Ag Surfaces. *ACS Catal.* **2015**, *5*, 4293−4299.

(28) Yoon, Y.; Hall, A. S.; Surendranath, Y. Tuning of Silver Catalyst Mesostructure Promotes Selective Carbon Dioxide Conversion into Fuels. *Angew. Chem., Int. Ed.* **2016**, *55*, 15282−15286.